A Possible Role of Solar Radiation and Ocean in the Mid-Holocene East Asian Monsoon Climate

WEI Jiangfeng*[1,2] (魏江峰), and WANG Huijun[1] (王会军)

[1] *Nansen-Zhu International Research Center, Institute of Atmospheric Physics, Chinese Academy of Sciences, Beijing* 100029

[2] *School of Earth and Atmospheric Sciences, Georgia Institute of Technology, Atlanta, GA* 30332-0340, *USA*

(Received 16 February 2003; revised 12 August 2003)

ABSTRACT

An atmospheric general circulation model (AGCM) and an oceanic general circulation model (OGCM) are asynchronously coupled to simulate the climate of the mid-Holocene period. The role of the solar radiation and ocean in the mid-Holocene East Asian monsoon climate is analyzed and some mechanisms are revealed. At the forcing of changed solar radiation induced by the changed orbital parameters and the changed SST simulated by the OGCM, compared with when there is orbital forcing alone, there is more precipitation and the monsoon is stronger in the summer of East Asia, and the winter temperature increases over China. These agree better with the reconstructed data. It is revealed that the change of solar radiation can displace northward the ITCZ and the East Asia subtropical jet, which bring more precipitation over the south of Tibet and North and Northeast China. By analyzing the summer meridional latent heat transport, it is found that the influence of solar radiation change is mainly to increase the convergence of atmosphere toward the land, and the influence of SST change is mainly to transport more moisture to the sea surface atmosphere. Their synergistic effect on East Asian precipitation is much stronger than the sum of their respective effects.

Key words: paleoclimate modeling, asynchronous coupling, mid-Holocene, East Asian climate, monsoon

1. Introduction

The megathermal period in the Holocene appeared during 8.5–3 ka BP (thousand years before present) with a maximum in 7.2–6 ka BP in China, when the temperature was 1–5°C higher and the precipitation was 40%–100% greater than present over China (Shi et al., 1992). What induced such a large climate change? According to Milankovitch theory (Milankovitch, 1941), the change of orbital parameters can lead to the change of insolation, which causes global climate change. The periodical change of orbital parameters is the main reason why glacial and interglacial periods alternate in the Quaternary. This theory has been supported by many paleoclimate records.

According to reconstructed data, the mid-Holocene change in boundary conditions was relatively small (COHMAP, 1988). Change in orbital forcing and reduction in CO_2 concentration are believed to be the principal contributors to the significant climate difference. But simulations with orbital parameters and CO_2 concentration as the changed boundary forcing have failed to reproduce the observed climate change quantitatively (Joussaume et al., 1999). Many researches have revealed that the changes of land surface characteristics (Charney et al., 1977; Nobre et al., 1991; Xue and Shukla, 1993) and ocean (Bjerknes, 1966; Rowntree, 1972; Palmer and Sun, 1985) have important effects on the climate change, and that there are feedbacks between them and the climate. With the improvement of climate models and increase of computer power in recent years, the impacts of vegetation, soil, and SST have been gradually taken into account in the paleoclimate modeling (Kutzbach et al., 1996; Claussen, 1997; Kutzbach and Liu, 1997; Hewitt and Mitchell, 1998; Doherty et al., 2000). Great advancement has been made and many mechanisms have been revealed.

Although these simulations are global, they mainly focus on the African monsoon area. Few diagnoses

*E-mail: jwei@eas.gatech.edu

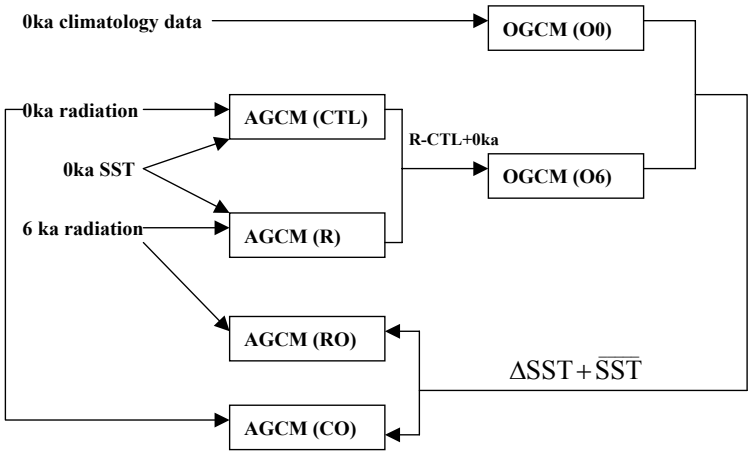

Fig. 1. The iteration sequence of the numerical experiments.

were done on the Asian monsoon area, especially the East Asian monsoon area, which we are most interested in. Former simulations with orbital change alone or changed orbital forcing and vegetation all produce characteristics like stronger summer monsoon and more precipitation in East Asia, but the magnitudes of the changes are underestimated (Wang, 1999). The reason is probably that the feedback of ocean to insolation change is not taken into account. In this paper, an AGCM and an OGCM are asynchronously coupled to simulate the climate of mid-Holocene. The role of solar radiation and ocean in the formation of the mid-Holocene East Asian monsoon climate is investigated, and some mechanisms are revealed.

2. Model and experiment design

2.1 *Model*

2.1.1 *Atmospheric model*

The AGCM we use in this paper was developed at the Institute of Atmospheric Physics (IAP), Chinese Academy of Sciences. It is a global grid point model with $4^\circ \times 5^\circ$ horizontal resolution and nine unequal levels in the vertical. The top layer is at 10 hPa. The land surface is divided into 10 vegetation types and 11 soil types. Forcing from the ocean is the climatological monthly mean SSTs (sea surface temperature). It has unique characteristics in model dynamics and computational scheme and has its own features in model physics. Detailed descriptions of the model can be found in Liang (1996) and Bi (1993).

2.1.2 *Oceanic model*

The OGCM used in this study was developed at IAP. It is a global model based on primitive equations. Its horizontal resolution is $4^\circ \times 5^\circ$ and it has 20 levels in the vertical, with 9 of them above 1000 m and the bottom is at 5000 m. When the predicted SST is below the freezing point, sea ice emerges. A simple thermodynamic sea ice model is formulated and incorporated into the ocean model based on Parkinson and Washington (1979). Detailed descriptions of the model can be found in Jin (2000).

2.2 *Experiment design*

2.2.1 *About the asynchronous coupling scheme*

The equilibrium asynchronous coupling scheme was first used by Kutzbach and Liu (1997), with detailed description given by Liu et al. (1999). In this scheme, each component model is integrated to its equilibrium before being coupled to the other component. Thus, it is an iterative coupling scheme between an equilibrium atmosphere and an equilibrium ocean. This scheme has two advantages. First, the oceanic model, which requires an enormous amount of computation time, can be integrated separately with a longer time step. This improves computational efficiency. Second, the individual equilibrium component experiments involve no ocean-atmosphere feedbacks, and therefore their response can be understood much more easily. This asynchronous coupling scheme is most effective only for the study of long-term climate change such as paleoclimate and global warming, rather than for short-term climate variability such as ENSO. According to Liu et al. (1999), in both summer and winter, the SST changes of the first and second iteration account for almost 3/4 and 1/4 of the total SST changes, respectively. Therefore, this scheme converges very quickly.

2.2.2 *Experiment design*

First, we force the AGCM with modern boundary conditions as the control run (experiment CTL). Then we change the orbital parameters to that of 6 ka BP (according to Paleoclimate Modelling Intercomparison

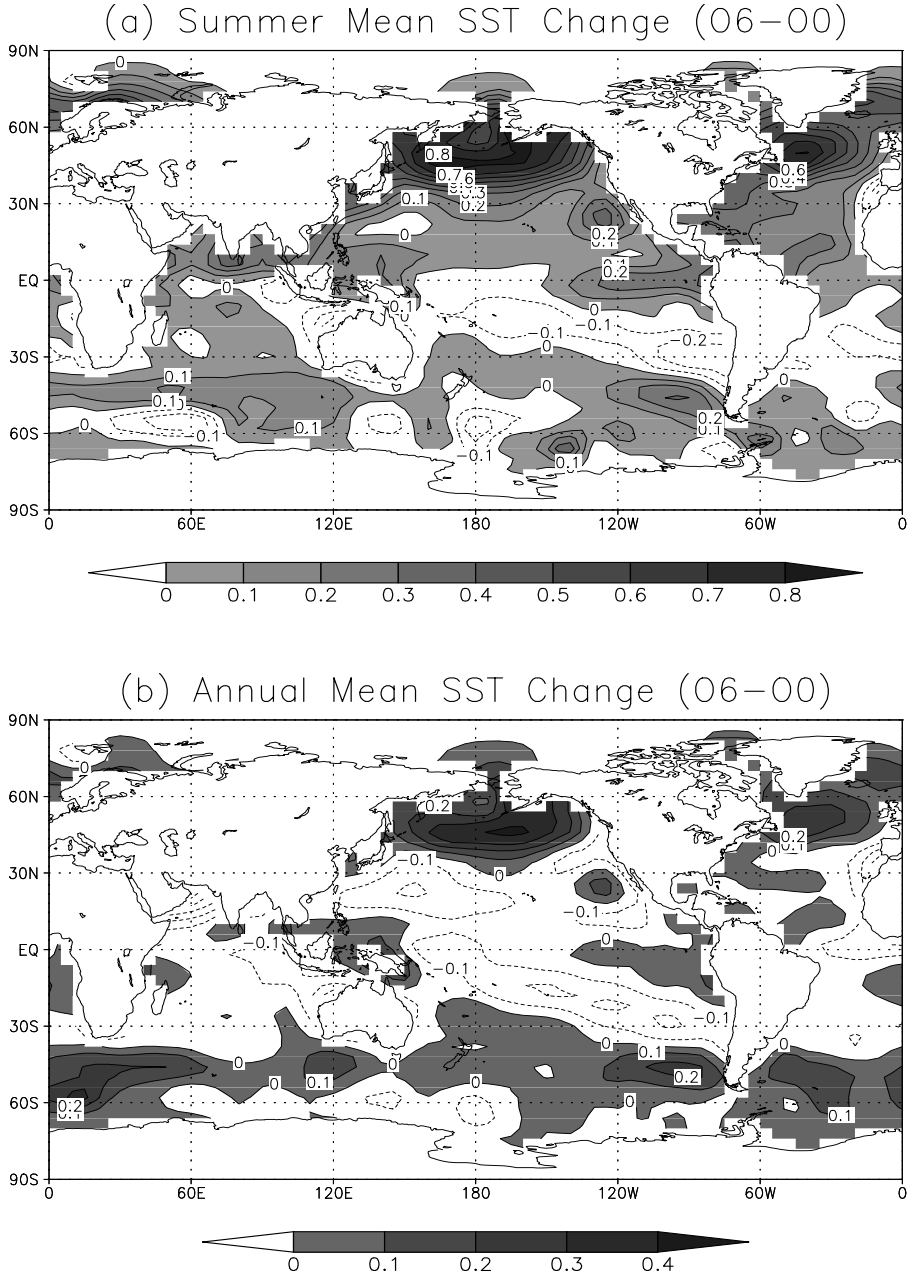

Fig. 2. The SST differences simulated by the OGCM (O6–O0) (°C). Areas with values larger than 0°C are shaded. (a) summer, (b) annual mean.

Project (PMIP)) with the other boundary forcing remaining unchanged. We thus obtain the response of the atmosphere to 6 ka BP radiation (experiment R). The differences of sea surface wind stress, wind velocity, sea surface pressure, temperature, surface water vapor mixing ratio, total cloud amount, and total downward solar radiation from the above two experiments are added to modern climatological fields to force the OGCM. So we obtian the response of the ocean to 6 ka BP radiation (experiment O6). The possible changes in salinity caused by the freshwater flux are ignored. The other OGCM experiment is the control run of ocean (experiment O0) in which the OGCM is forced with the modern climatological fields. Then we compute the SST difference of experiment O6 and O0 and add it to the modern climatological SST fields to force the AGCM together with 6 ka BP radiation. We thus obtain the response of the atmosphere to 6 ka

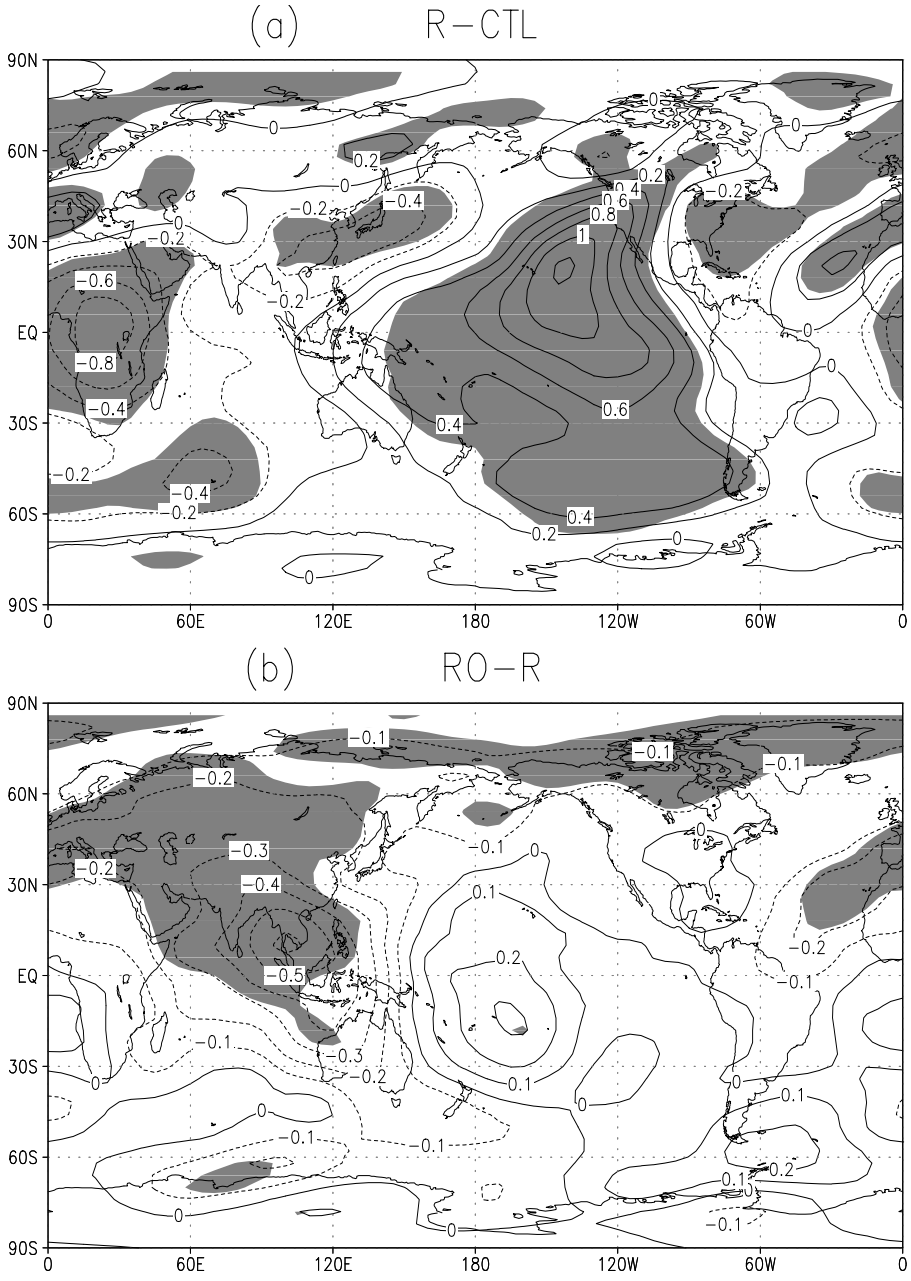

Fig. 3. The changes of summer (JJA) 200-hPa velocity potential (10^6 m^2 s^{-1}). (a) The influence of orbital change (R–CTL), (b) the influence of SST change (RO–R). Negative values indicate divergence. Areas with significance level at 95% are shaded.

BP radiation and SST (experiment RO). Possible changes of sea ice cover are ignored. Another AGCM experiment is the response of the atmosphere to 6 ka BP SST (experiment CO) in which the SST forcing is the same as experiment RO and other forcings are the same as the control run.

The experiment design includes only one iteration, because the first iteration accounts for most of the SST changes. We use the method of adding the difference of two experiments to the climatological fields in order to decrease the system biases of the models. The AGCM and OGCM are integrated for 14 and 3010 years respectively. The ensemble averages of the last 13 and 10 years are calculated as equilibrium results of the models. The iteration sequence is shown schematically in Fig. 1.

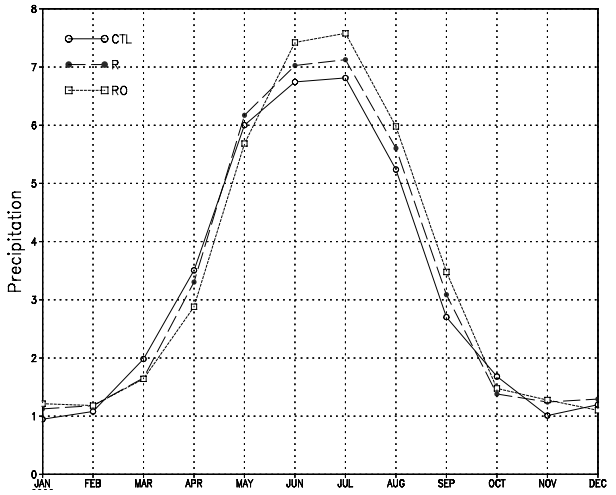

Fig. 4. The seasonal variation of East Asian precipitation in the three experiments CTL, R, and RO (mm d^{-1}).

3. Simulated main characteristics of East Asian climate change

Figure 2 shows the SST differences between experiment O6 and O0. In both summer (June, July, and August JJA hereafter) and annual mean, the strongest warming is located in the northern high latitudes, and there is some warming on the southern sea surface. It warms little and even cools in the tropics. The SST changes in the tropics agree qualitatively with the reconstructions of Gagan et al. (1998) and Andrus et al. (2002), but the magnitudes are underestimated.

The summer (JJA) 200-hPa velocity potential changes are given in Fig. 3. Under the influence of the 6 ka BP radiation (R–CTL), there is more divergence in the high levels (Fig. 3a) and more convergence in the low levels in East Asia. As a result, there is more ascending motion and more precipitation (Fig. 5a). The SST change (RO–R) further strengthens the effect. There is a large area of divergence increase around the South China Sea at 200 hPa (Fig. 3b).

Figure 4 shows the seasonal variation of East Asian precipitation in the three experiments CTL, R, and RO. In summer (JJA), the precipitation of R is larger than that of CTL, and RO is larger than R. We can see that when we take into account the effect of ocean, the East Asian monsoon is stronger and the simulated results are closer to the reconstructions (Shi et al., 1992). The distribution of summer (JJA) precipitation changes can be seen in Fig. 5. The orbital change of 6 ka BP leads to more precipitation over the south of Tibet and North and Northeast China (Fig. 5a). Under the influence of SST change, there is more precipitation over South and East China while there is less precipitation over North China, although it does not pass the significance level, which may be a result of large interannual variability of precipitation in East Asia.

The 6 ka BP orbital change enhances the seasonal cycle of Northern Hemisphere insolation (Berger, 1978). This would lead to the warming of northern summer-autumn (Fig. 6a) and cooling of northern winter-spring (figures not shown). While under the influence of SST change (RO–R), the northern summer cools (Fig. 6b) and the China inland winter warms (figures not shown). This is due to the huge thermal inertia of ocean and will be further discussed in a later section. According to the geological record of mid-Holocene (Shi et al., 1992), there has been large warming in winter over China, and its magnitude was larger than that of summer. So introducing the influence of ocean brings the simulated and reconstructed results into closer agreement. But the winter temperature still decreases. This is perhaps due to the fact that there are other physical processes not accounted for, such as the response and feedback of sea ice and vegetation to climate change.

Figure 7 shows the summer (JJA) 85°–122°E mean meridional wind circulation. We can see obvious summer Hadley circulation in the climatological run (Fig. 7a). The place where the Hadley circulation has the strongest rising is the place of the ITCZ. Under the influence of changed solar radiation (R–CTL), there is increased sinking at about 10°N, and increased rising at 20°–30°N (Fig. 7b), which suggests that the place of strongest rising (the place of the ITCZ) moves northward.

Under the influence of SST change (RO–R), both the Northern Hemisphere Hadley circulation (Fig. 7c) and Pacific Walker circulation (figures not shown) become stronger. The changes of the Hadley and Walker circulations reflect the divergence and convergence differences between the north and south, east and west (Fig. 3b).

4. Mechanisms of East Asian climate change

4.1 *Influences of solar radiation*

Under the influence of changed solar radiation, it is drier in the south of the Indian peninsula and Indochina and wetter to the south of the Tibet (Fig. 5a). This is because the change of solar radiation leads to the warming of the Northern Hemisphere in summer (Fig. 6). Under the heating of Tibet, the ITCZ moves northward (Figs. 7a, b).

There is more precipitation in the north to the east of 105°E (Fig. 5a). It is caused by the northward displacement of the East Asian jet stream (Figs. 7a, b).

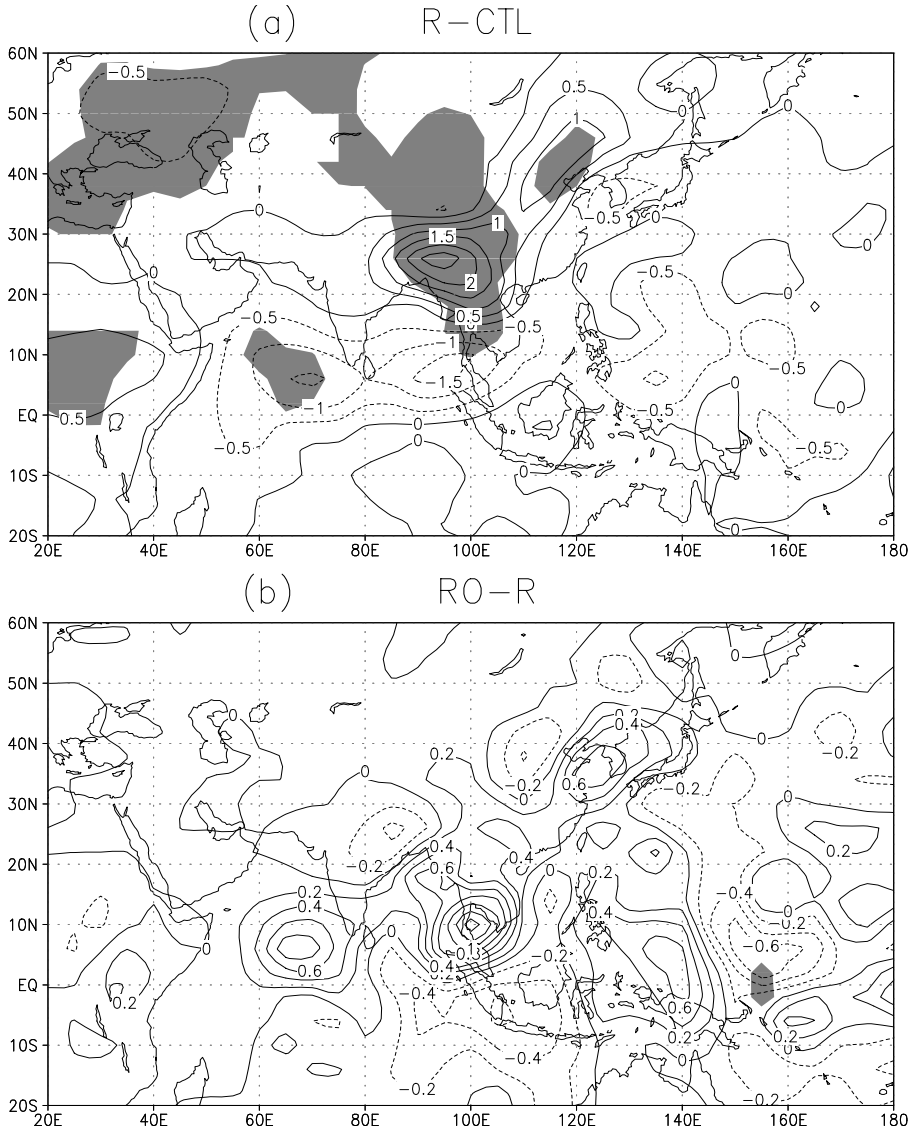

Fig. 5. Same as Fig. 3, but for the summer (JJA) precipitation (mm d^{-1}).

The association between rainfall bands and tropospheric jet streams has long been recognized (Reiter, 1963). The north-south displacement of the Asian westerly jet is a reliable indicator of Asian monsoon onset and retreat (Yeh et al., 1958). This subtropical jet in East Asia is formed in the large temperature gradient made by the polar continental air mass in the north, and the warm and wet air mass in the south. The orbitally-induced heating in the northern continent northward displaces the area of maximum temperature gradient in the upper level (figures not shown), thus it displaces the jet stream northward. There is descending motion at the north of the jet stream and ascending motion at the south. Descending motion prohibits rain to the north of the jet core. Thus there is more ascending motion in the areas where the jet core leaves (35°–45°N) (Fig. 7b), and hence more precipitation (Fig. 5a).

On the other hand, under the influence of orbital change, the total amount of precipitation changes very little in the Asian monsoon area (decreased by about 2.7% in 0°–50°N, 60°–140°E). This result is similar to that of De Noblet et al. (1996). They found that the location and intensity of simulated precipitation maxima are very sensitive to change in insolation, while the total amount of monsoon rain in Asia as well as Africa remains remarkably stable. This may be because there is no moisture transport increase when SST remains unchanged.

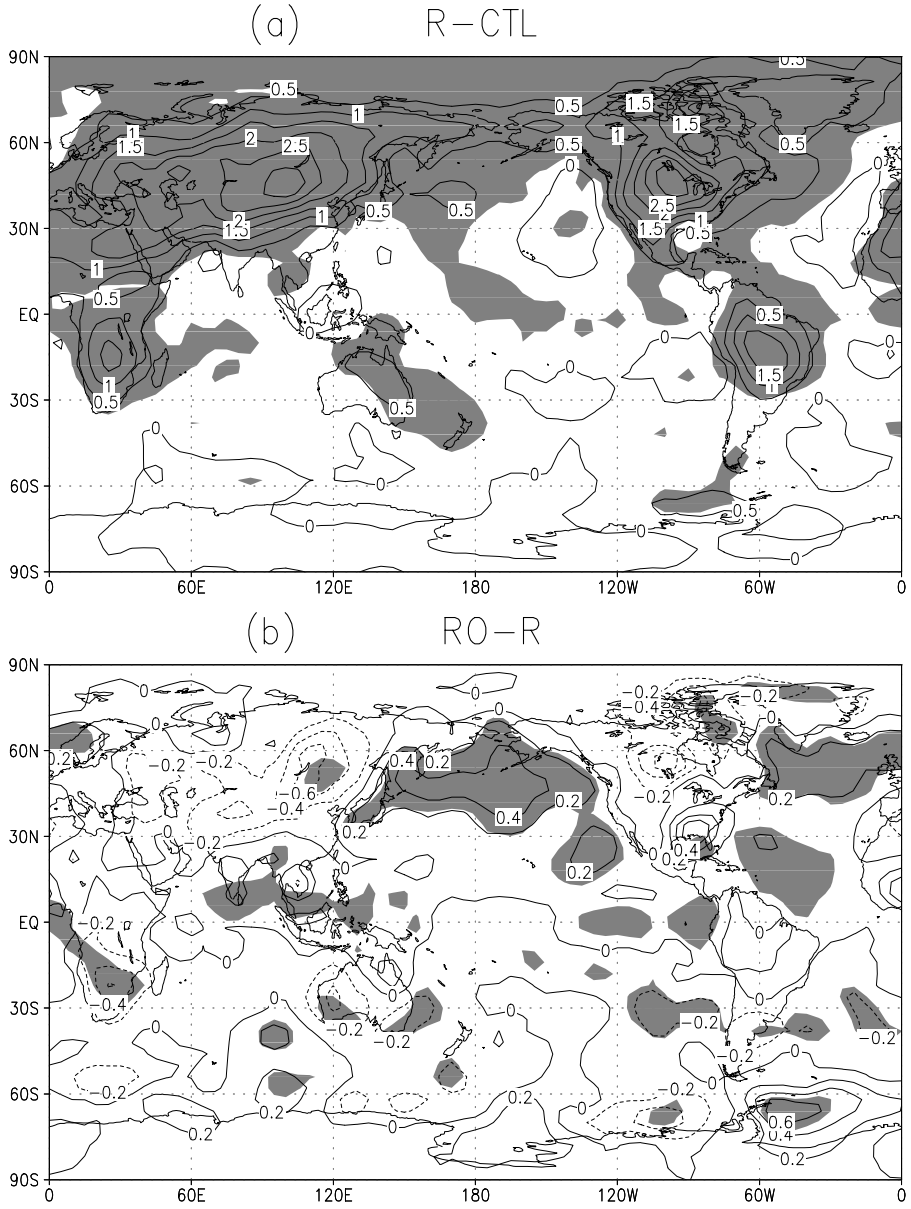

Fig. 6. Same as Fig. 3, but for the summer (JJA) surface temperature (°C).

4.2 *Influence of ocean*

Ocean has its unique characteristics and is a very important component of the earth climate system. Only when we fully understand the dynamics of ocean-atmosphere interaction, can we accurately predict the climate with high accuracy.

Figure 8 shows the sensible heat flux difference (RO–R) from the earth's surface to the atmosphere. It is the sensible heat flux change when taking into account the SST change. We can see that the centers of large values are mainly on the sea surface, and they correspond well with the large value centers of SST change in Fig. 2a. This sensible heat difference is caused by the change of SST. On the other hand, the centers of sensible heat difference in Fig. 8 correspond well with the cyclonic centers of surface wind difference (figures not shown). When sensible heat increases, it heats the surface atmosphere. Then the pressure decreases and cyclonic circulation becomes stronger.

The SST change not only induces sensible heat flux change, but also induces latent heat flux change. The latent heat flux cannot change the temperature of the atmosphere directly, but it can be converted into heat by coagulation and heat the atmosphere, and it is usually much larger than the sensible heat flux. It can be

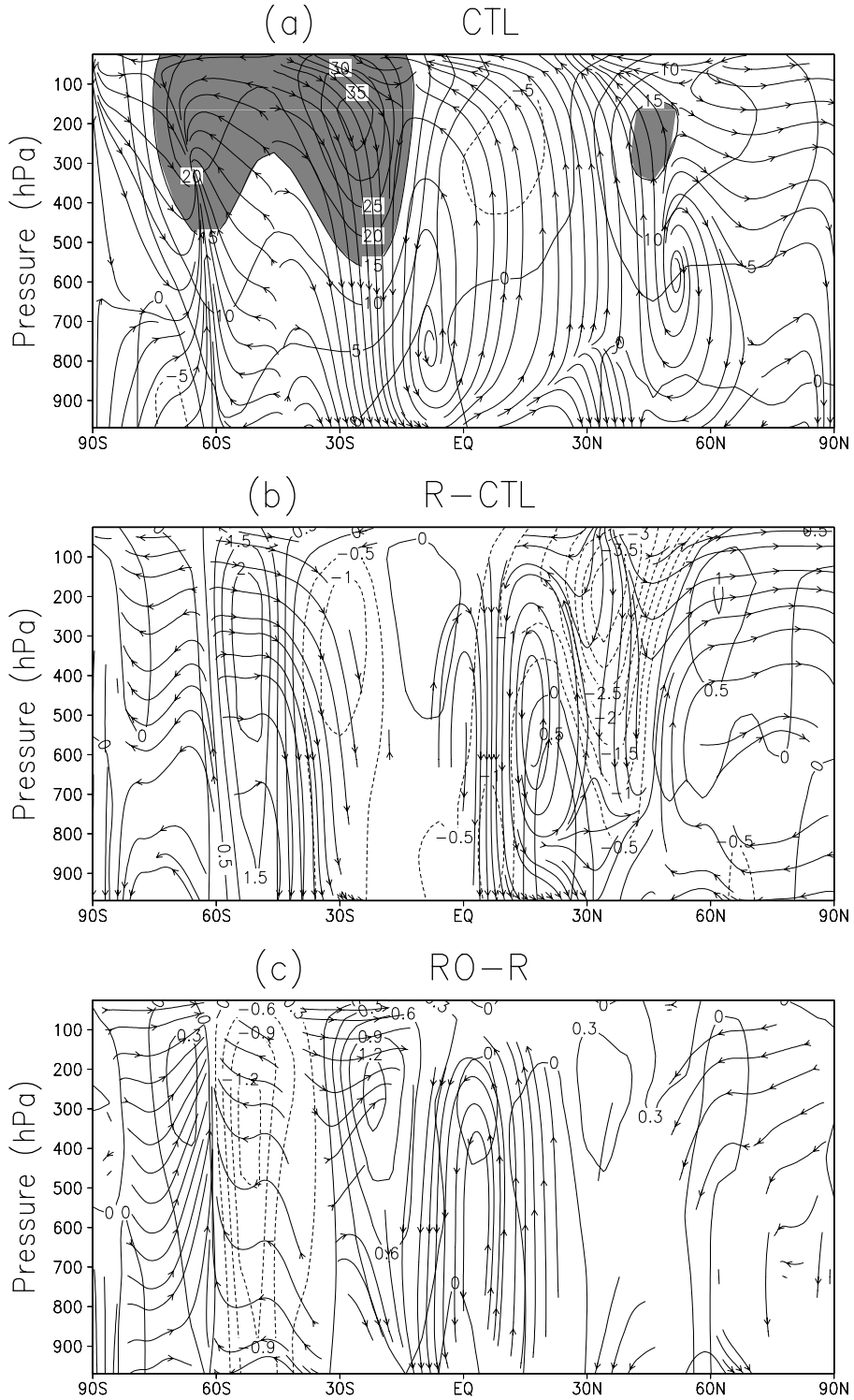

Fig. 7. The summer (JJA) 85°–122°E mean meridional wind circulation. The zonal ($m\,s^{-1}$) and meridional ($m\,s^{-1}$)/vertical (10^{-4} $hPa\,s^{-1}$) components are represented by contours and vectors respectively. Areas with zonal wind larger than 15 $m\,s^{-1}$ are shaded. (a) Control run (CTL), (b) the influence of orbital change (R–CTL), (c) the influence of SST change (RO–R).

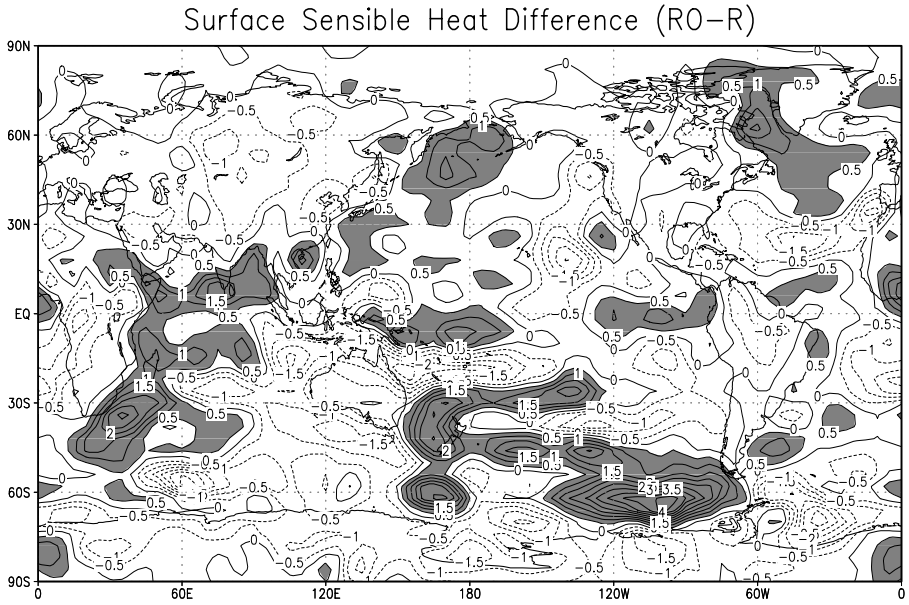

Fig. 8. The sensible heat flux difference between experiment RO and R from the earth's surface to the atmosphere ($\mathrm{W\,m^{-2}}$). Areas with values larger than $0.5\,\mathrm{W\,m^{-2}}$ are shaded.

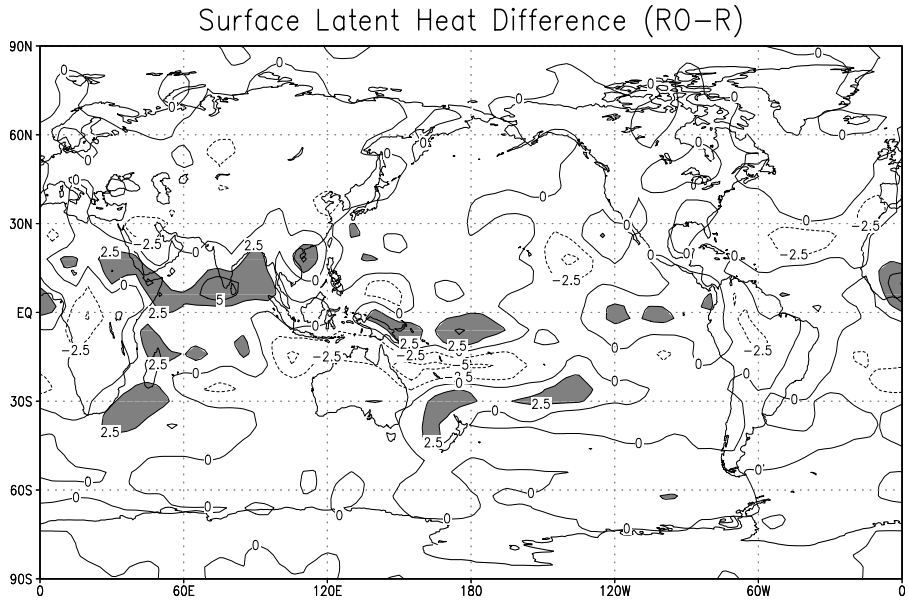

Fig. 9. The latent heat flux difference between experiment RO and R from the earth's surface to the atmosphere ($\mathrm{W\,m^{-2}}$). Areas with values larger than $2.5\,\mathrm{W\,m^{-2}}$ are shaded.

seen that the large value centers of latent heat flux changes (Fig. 9) correspond well with the large value centers of convective precipitation change (figures not shown). So we think that the role of sensible heat flux on the sea surface is to excite convection, while the role of latent heat is to maintain and increase convection. The maintenance and development of convection needs the continuous support of latent heat. When convection happens, the latent heat is transformed into heat and warms the atmosphere, and promotes convection continuously by the conditional instability of second kind (CISK) mechanism.

4.3 *Synergistic effect of solar radiation and ocean*

The summer (JJA) precipitation changes in East

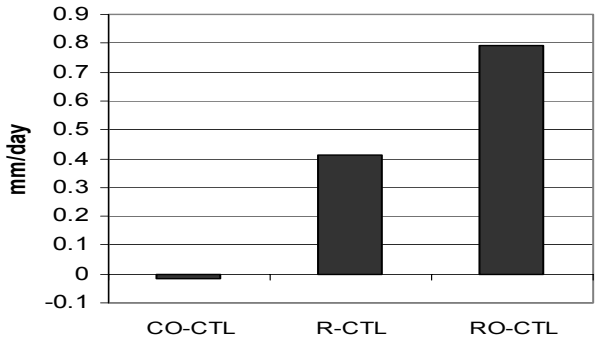

Fig. 10. The histogram of summer mean precipitation changes in East Asia (20°–40°N, 105°–120°E) (mm d^{-1}).

Asia at three different forcings can be seen in Fig. 10. The SST change alone (CO–CTL) contributes little to precipitation change. Under the influence of solar radiation change alone (R–CTL), the summer mean precipitation increases by 0.41 mm d^{-1}. While under the combined influence of solar radiation and SST change, the precipitation increase is 0.79 mm d^{-1}, which is much larger than the sum of their respective effects. This indicates that the synergistic effect of solar radiation and SST change plays an important role in East Asian precipitation increase. Now we analyze how this happens.

Because the latent heat transport has a close relationship to rainfall, we can analyze the difference of latent heat transport in the experiments to reveal the mechanisms of precipitation changes. Figure 11 shows the summer (JJA) meridional latent heat transport in the whole atmosphere over East Asia. The figure contains the results of four experiments. In the tropics, RO is larger than R and CO is larger than CTL. In the subtropics, the differences are not evident between RO and R, and CO and CTL, while there are large differences between R and CTL, and RO and CO. This indicates that the tropical ocean has much influence on the meridional latent heat transport in the tropics, while in the subtropics the solar radiation has a larger influence. When SST increases in the Bay of Bengal and the South China Sea which are in the tropics, evaporation enhances on the sea surface, and more moisture goes from ocean to atmosphere, so the latent heat transport is increased. In the subtropics, the increased solar radiation in summer warms the land and the surface pressure decreases, so there is more convergence on the land and more divergence on the sea surface (Fig. 3a), which promote the inland transport of moisture and latent heat.

The formula of meridional latent heat transport is

$$F = \int\int \frac{Lqv}{g} dpdx \,, \qquad (1)$$

in which F is meridional latent heat transport, L is evaporation latent heat, q is specific humidity, v is meridional velocity, g is gravitational acceleration, and dp and dx are the integration factors of vertical pressure and zonal distance respectively. According to the analyses above, the influence of orbital change is to promote the convergence of atmosphere inland, i.e. increase v, and the influence of SST change is mainly to transport more moisture to the sea surface atmosphere, i.e., increase q. They combine together to increase the latent heat transport F.

Let v' be the orbitally-induced meridional velocity increase and q' be the SST change-induced specific humidity increase (in the area studied $v' > 0$, $q' > 0$), if the integration process above is omitted and we only study the term qv, we can get:

(1) The contribution of orbital change alone to latent heat transport is $F_s = q(v + v') - qv = qv'$;

(2) The contribution of SST change alone to latent heat transport is $F_o = (q + q')v - qv = q'v$;

(3) The combined contribution of orbital change and SST change to latent heat transport is $F_{so} = (q + q')(v + v') - qv = qv' + q'v + q'v'$.

Evidently, $F_{so} > F_o + F_s$. This is why the synergistic effect of the solar radiation and ocean on East Asian precipitation is much stronger than the sum of their respective effects.

5. Summary and discussion

We use the asynchronous coupling technique to simulate the climate of mid-Holocene, and analyze the role of solar radiation and ocean in the mid-Holocene East Asian monsoon climate and their synergistic influence on climate change.

A coupled ocean-atmosphere general circulation model (CGCM) has not been used before in East Asian paleoclimate modeling. The orbital change or orbital and vegetation change are the usually prescribed boundary forcing. SSTs are prescribed as modern climatological fields. But under such a large solar radiation change, it is not possible for the SSTs to remain unchanged. The ocean occupies most of the earth's surface and is the main source of moisture in the atmosphere. So introducing an OGCM in the paleoclimate modeling will make the physical processes more complete and the simulations more accurate. According to the analysis of East Asian summer precipitation, the precipitation change induced by the combined influence of orbital and SST changes is almost twice of the precipitation change induced by the orbital change alone (Fig. 10), which agrees more with reconstructions. However, the OGCM requires too much com-

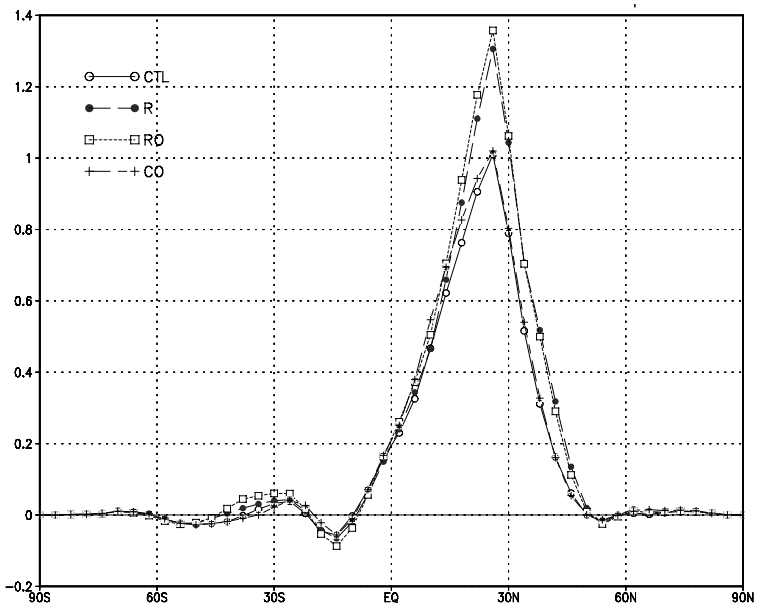

Fig. 11. The summer meridional latent heat transport in the whole atmosphere in 100°–120°E. Units: 10^{15} W. Positive values indicate northward transport.

putation time, especially when taking a long time integration and when many sensitivity experiments are needed. The results may be too complex to understand the underlying processes. The asynchronous coupling scheme we use solves the problems quite well.

There is only one iteration in this study. If there are more iterations, will there be some nonlinear progresses which will change the results qualitatively? We did not allow for consideration of possible changes in salinity associated with changes in freshwater flux, sea ice, and vegetation changes induced by insolation changes. If all these changes are considered, will their synergistic effect make the East Asian monsoon stronger and bring the simulated and reconstructed results into closer agreement? All these questions need further study.

Changing the date of perihelion from early January to mid-September in mid-Holocene increases the amplitude of the seasonal cycle of Northern Hemisphere insolation by 5% (Berger, 1978), which leads to enhanced heating in northern summer-autumn and enhanced cooling in northern winter-spring. If the reconstructed result of winter warming is correct, what are the mechanisms of the warming? Ganopolski et al. (1998) simulated mid-Holocene climate with a synchronously coupled atmosphere-ocean-vegetation model. The results show a winter warming in the Northern Hemisphere. The warming is caused by a decrease of planetary albedo due to an expansion of boreal forest and a decrease of subtropical deserts. In high northern latitudes, warming is strongly amplified by the sea-ice feedback. The annual amount of sea ice decreased by one-quarter compared to present. As a result, the ocean absorbs more heat in summer and releases it into the atmosphere in autumn and winter. Thus the land surface characteristics and ocean play important roles in the mid-Holocene climate. Designing coupled atmosphere-ocean-land models involving interactions of atmosphere, land surface, and ocean with more detailed physics and higher resolutions is what we should do in our future work. This will surely reveal more mechanisms of climate change.

Acknowledgments. This research was supported by the National Outstanding Youth Foundation under Grant No. 40125014, and the Chinese Academy of Sciences Key Project under Grant KZCX3-AW-133. The authors thank Dr. Yu Yongqiang for his assistance in the use of IAP OGCM.

REFERENCES

Andrus, C., F. T. Fred, D. E. Crowe, D. H. Sandweiss, E. J. Reitz, and C. S. Romanek, 2002: Otolith δ^{18}O record of mid-Holocene sea surface temperatures in Peru. *Science*, **295**, 1508–1511.

Berger, A. L., 1978: Long-term variations of daily insolation and quaternary climate change. *J. Atmos. Sci.*, **35**, 2362–2367.

Bi Xunqiang, 1993: The IAP 9-level AGCM and the climate simulation. Ph. D. dissertation, Institute of Atmospheric Physics, Chinese Academy of Sciences, Beijing. (in Chinese)

Bjerknes, J., 1966: A possible response of the atmospheric Hadley circulation to equatorial anomalies of ocean temperature. *Tellus*, **18**, 820–829.

Charney, J., W. J. Quirk, S. H. Chow, and J. Kornfield, 1977: A comparative study of the effect of albedo change on drought in semi-arid regions. *J. Atmos. Sci.*, **34**, 1366–1358.

Claussen, M., 1997: Modeling bio-geophysical feedback in the African and Indian Monsoon region. *Climate Dyn.*, **13**, 247–257.

COHMAP members, 1988: Climate changes of the last 18,000 years: Observations and model simulations. *Science*, **241**, 1043–1052.

De Noblet, N., P. Braconnot, S. Joussaume, and V. Masson, 1996: Sensitivity of simulated Asian and African summer monsoons to orbitally induced variations in insolation 126, 115 and 6 kBP. *Climate Dyn.*, **12**, 589–603.

Doherty, R., J. Kutzbach, J. Foley, and D. Pollard, 2000: Fully coupled climate/dynamical vegetation model simulations over northern Africa during the mid-Holocene. *Climate Dyn.*, **16**, 561–573.

Gagan, M. K., L. K. Ayliffe, and D. Hopley, 1998: Temperature and surface-ocean water balance of the mid-Holocene tropical western Pacific. *Science*, **279**, 1014–1018.

Ganopolski, A., C. Kubatzki, M. Claussen, V. Brovkin, and V. Petoukhov, 1998: The influence of vegetation-atmosphere-ocean interaction on climate during the mid-Holocene. *Science*, **280**, 1916–1919.

Hewitt, C., and J. F. B. Mitchell, 1998: A fully coupled GCM simulation of the climate of the mid-Holocene. *Geophys. Res. Lett.*, **25**, 361–364.

Jin Xiangze, Zhang Xuehong, and Yu Yongqiang, 2000: Oceanic general circulation and sea ice model. *IAP Global Ocean-Atmosphere-Land System Model*, Zhang Xuehong, Wu guoxiong, Yu Yongqiang, and Jin Xiangze, Eds., Science Press, Beijing, 76–99.

Joussaume, S., 1999: Monsoon changes for 6000 years ago: Results of 18 simulations from the Paleoclimate Modeling Intercomparison Project (PMIP). *Geophys. Res. Lett.*, **26**, 859–862.

Kutzbach, J., G. Bonan, J. Foley, 1996: Vegetation and soil feedbacks on the response of African monsoon to orbital forcing in the early to middle Holocene. *Science*, **348**, 623–626.

Kutzbach, J., and Z. Liu., 1997: Response of the African monsoon to orbital forcing and ocean feedbacks in the Middle Holocene. *Science*, **278**, 440–443.

Liang Xinzhong, 1996: Description of a nine-level grid point atmospheric general circulation model. *Adv. Atmos. Sci.*, **13**, 269–298.

Liu, Z., R. G. Gallimore, J. E. Kutzbach, W. Xu, Y. Golubev, P. Behling, and R. Selin, 1999: Modeling long-term climate changes with equilibrium asynchronous coupling. *Climate Dyn.*, **15**, 325–340.

Milankovitch, M., 1941: Kanon der Erdbestrahlung and seine Anwendung anf desEiszeitenproglen. *Academic Royale Serbe*, Belgrade, Special Edition, 133pp. (in Yugoslavian)

Nobre, C. A., P. J. Sellers, and J. Shukla, 1991: Amazonian deforestation and regional climate change. *J. Climate*, **4**, 957–988.

Palmer, T. N., and Z. Sun, 1985: A modeling and observational study of the relation between sea surface temperature in the North-west Atlantic and the atmospheric general circulation. *Quart. J. Roy. Meteor. Soc.*, **111**, 947–975.

Parkinson, C. L., and W. M. Washington, 1979: A large scale numerical model sea ice. *J. Geophys. Res.*, **84**, 311–337.

Reiter, E. R., 1963: *Jet-stream Meteorology.* University of Chicago Press, 515pp.

Rowntree, P. R., 1972: The influence of tropical East Pacific ocean temperature on the atmosphere. *Quart. J. Roy. Met. Soc.*, **98**, 290–321.

Shi Yafeng, and coauthors, 1992: The general characteristics of mid-Holocene climate and environment over China. *Mid-Holocene Climate and Environment over China*, Shi Yafeng and Kong Zhaochen, Eds., China Ocean Press, Beijing, 1–18. (in Chinese)

Wang, H. J., 1999: Role of vegetation and soil in the Holocene megathermal climate over China. *J. Geophys. Res.*, **104**(D8), 9361–9367.

Xue, Y., and J. Shukla, 1993: The influence of land surface properties on Sahel climate. Part I: Deforestation. *J. Climate*, **6**, 2232–2245.

Ye Duzheng, Tao Shiyan, and Li Maicun, 1958: The abrupt phenomenon of the general atmospheric circulation in June and October. *Acta Meteorologica Sinica,* **29**, 246–263. (in Chinese)